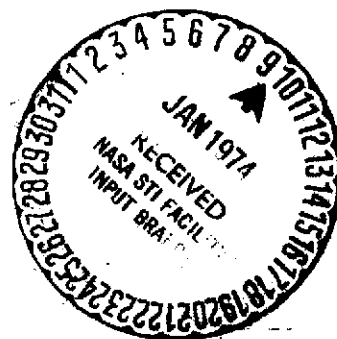


NATIONAL AERONAUTICS AND SPACE ADMINISTRATION

*Technical Report 32-1591*

*Conical Quadreflex Antenna Analytical Study*

*Paul W. Cramer, Jr.*



(NASA-CR-136279) CONICAL QUADREFLEX  
ANTENNA ANALYTICAL STUDY (Jet Propulsion  
Lab.) 10 p HC \$3.00 CSCL 17B  
1/

N74-12920

G3/09 Unclass  
24863

**JET PROPULSION LABORATORY  
CALIFORNIA INSTITUTE OF TECHNOLOGY  
PASADENA, CALIFORNIA**

December 15, 1973

NATIONAL AERONAUTICS AND SPACE ADMINISTRATION

*Technical Report 32-1591*

*Conical Quadreflex Antenna Analytical Study*

*Paul W. Cramer, Jr.*

JET PROPULSION LABORATORY  
CALIFORNIA INSTITUTE OF TECHNOLOGY  
PASADENA, CALIFORNIA

December 15, 1973

Prepared Under Contract No. NAS 7-100  
National Aeronautics and Space Administration

## **Preface**

The work described in this report was performed by the Telecommunications Division of the Jet Propulsion Laboratory.

# Contents

I. Introduction . . . . .	1
II. Geometrical Optics . . . . .	2
III. Efficiency Determined by Scattering Calculations . . . . .	5
References . . . . .	5

## Table

1. Antenna efficiency . . . . .	5
---------------------------------	---

## Figures

1. Quadreflex geometry . . . . .	1
2. Equivalent parabola configuration . . . . .	3
3. Horn pattern required to produce uniform aperture illumination by ray tracing . . . . .	3
4. Exponential feed patterns for quadreflex antenna . . . . .	3
5. Aperture fields for quadreflex antenna . . . . .	3
6. Spillover, illumination, and overall efficiencies of quadreflex antenna . . . . .	4
7. Flow diagram of computer programs for calculating efficiency . . . . .	4
8. Subreflector and feed parameters . . . . .	4

## **Abstract**

Conical antennas have recently been shown to effectively meet the requirements for large erectable spacecraft antennas. One configuration investigated consists of an antenna with three scattering surfaces requiring four reflections for an electromagnetic wave. This article presents a method for evaluating the performance of a four-reflection or "quadreflex" antenna. Geometrical optics was used initially to determine the ideal feed pattern required to produce uniform illumination on the aperture of the conical reflector and the reverse problem of quickly finding the aperture illumination given an arbitrary feed pattern. The knowledge of the aperture illumination makes it possible to compute the antenna efficiency, which is useful for comparing antenna performance during tradeoff studies. Scattering calculations, using physical optics techniques, were then used to more accurately determine the performance of a specific design.

# Conical Quadreflex Antenna Analytical Study

## I. Introduction

The conical quadreflex antenna is a four-reflection antenna consisting of a feed horn, ellipse of revolution sub-reflector, an "urn" with a parabola of revolution shape, and a conical reflector (Fig. 1) (Refs. 1 and 2).

In its simplest form, the antenna can be considered to consist of an equivalent parabola which generates a surface by being rotated about an axis parallel to and offset from the axis of parabola. The focus of the surface thus generated is a ring formed by the focus of the parabola as it is rotated about the offset axis. The ellipse serves the purpose of transforming a point focus on the axis of rotation to the ring focus required by the equivalent parabola of revolution.

The antenna has one unique feature which complicates the design procedure. The pattern illuminating the urn-conical surface structure is inverted from the original feed pattern. This can be visualized by referring to Fig. 1. Beginning with the feed at the focus point, an axial ray 1-2 is scattered from the ellipse as ray 2-3, which becomes rays 3-4, 4-5, and 5-6 in sequence. An off-axis ray 1-8 from

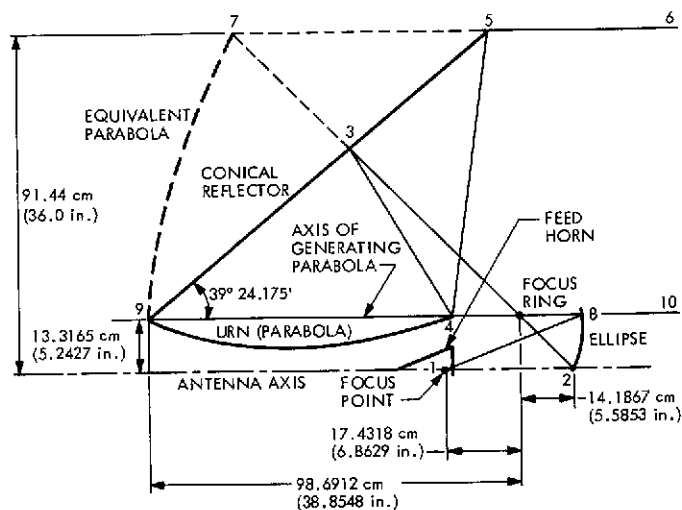


Fig. 1. Quadreflex geometry

the feed becomes rays 8-9, 9-9, 9-9, and 9-10. Thus, the outer ray from the feed becomes the inner ray after final scattering from the antenna.

This phenomenon causes a number of design problems since the traditional edge taper problem is now affecting

the performance of the center of the equivalent parabola and the center of the feed pattern, which contains little of the pattern power due to the  $\sin \theta$  effect, is now illuminating the outer portions of the equivalent parabola, which accounts for a large part of the scattering surface area. The outer edge of the surface, therefore, experiences an unusually high level of edge taper. Therefore, it is necessary to determine the effect of this property on the antenna performance.

In the following discussion an equivalent parabolic surface will be used to replace the urn and conical reflector to simplify this analysis.

To facilitate the analysis of such an antenna, two techniques were used:

- (1) Geometrical optics was used as a fast and efficient tool for trade-off studies.
- (2) Scattering calculations were made on the 1.83-m (6-ft) version at 16.33 and 8.448 GHz to obtain a more accurate determination of the antenna performance.

## II. Geometrical Optics

Two objectives were to be met:

- (1) Given the quadreflex antenna configuration, determine the feed pattern required to provide a uniform amplitude aperture distribution. The feed phase pattern is constant since the antenna geometry of the quadreflex antenna transforms a spherical phase front from a feed into a uniform phase pattern on the aperture. Thus, the phase pattern transformation is defined and need not be determined.
- (2) Conversely, given practical feed patterns, determine what aperture plane distributions will result and what aperture efficiencies can be obtained. Again, due to the antenna geometry, for each ray originating from the feed, the phase where these rays intercept the aperture will differ from the feed phase by a constant. Thus, the phase transformation is simply defined.

To meet these two objectives, by ray optics, an expression was derived which related the aperture amplitude fields with the feed pattern:

$$E_A(r) = E_F(\theta) \frac{\sin(\phi - \theta)}{\sin(\phi + \beta) \sec\left(\frac{\beta}{2}\right)} \left| \frac{A \left\{ \frac{\sin(\phi + \beta)}{\sin(\phi - \theta)} + 1 \right\} - 2a \sin \beta}{2aF \left\{ A + 2F \tan\left(\frac{\beta}{2}\right) \right\}} \right|^{\frac{1}{2}} \quad (1)$$

where

$E_A(r)$  = aperture fields

$E_F(\theta)$  = feed pattern

and

$$0 = \cos \beta - \frac{\sin \beta (\cos \phi - M \cos \theta) + \sin \phi \cos \theta - \cos \phi \sin \theta}{M \sin \theta - \sin \phi} \quad (2)$$

Equation (2) must be solved for  $\beta = f(\theta)$ , where the aperture fields are desired, and  $\theta = g(\beta)$ , where the feed pattern is to be obtained. The parameters of these equations are defined in Fig. 2. A program entitled "Conical Quadreflex Antenna Efficiency Program" has been written to evaluate Eq. (1) and a program entitled "Transcendental Equation Solving Program" has been written to evaluate Eq. (2). It should be pointed out in Eq. (1) that the independent variable is either  $E_F(\theta)$  and its associated polar angle  $\theta$  or, by simple rearrangement,  $E_A(r)$  and its associated radius  $r$ .  $\phi$ ,  $A$ ,  $a$ , and  $F$  are fixed parameters defining the antenna geometry.  $r$ ,  $\theta$ , and  $\beta$  are functions



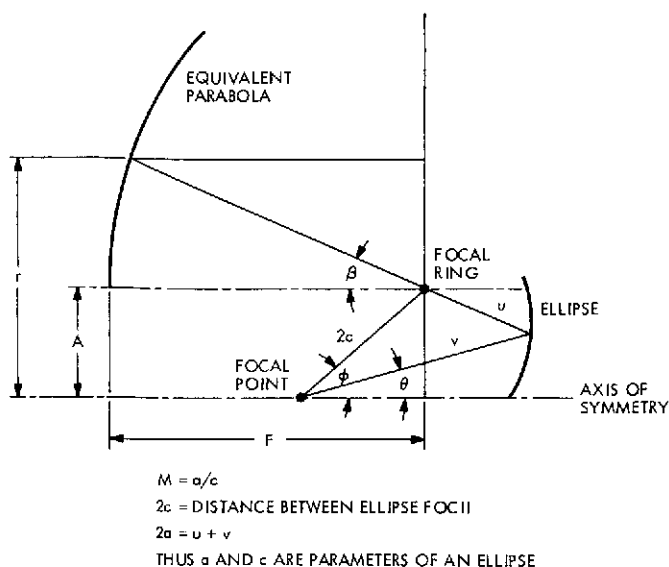


**Fig. 2. Equivalent parabola configuration**

of each other as shown by Eq. (2) and by the following expression:

$$r = A + 2F \tan \left( \frac{\beta}{2} \right) \quad (3)$$

The computed optimum feed pattern for a uniform aperture distribution is shown in Fig. 3. The infinite peak required on the axis is the result of the pattern inversion property of the quadreflex antenna and can be visualized as the zero area of the feed pattern center being required to illuminate the finite area of the outer edge of the conical reflector.

Utilizing Eq. (1) the aperture distribution was computed for an  $E = \exp(-K\theta^2)$  feed pattern. The exponential form was selected as it quite closely models the fields of the corrugated feed horn utilized in the quadreflex antenna. The parameter  $K$  is determined by the subreflector edge illumination desired. Figure 4 illustrates typical computed feed patterns selected to give edge tapers of 8 to 24 dB on the subreflector edge. The corresponding aperture distributions are shown in Fig. 5. It should be pointed out that in Fig. 5 the aperture fields were plotted as a function of the polar angle  $\beta$  (Fig. 2). Since  $\beta = 0$  is the center of the plot and corresponds to a point on the aperture a distance  $A$  from the axis of the antenna, the hole or null that appears in the aperture distribution within the radius  $A$  does not show in Fig. 5. If the fields had been plotted as a function of the radius  $r$ , the hole would not be suppressed, since the region within  $A$  would appear on the plot.

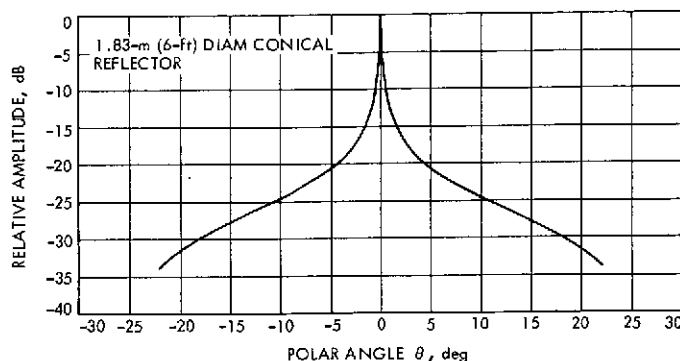


**Fig. 3. Horn pattern required to produce uniform aperture illumination by ray tracing**

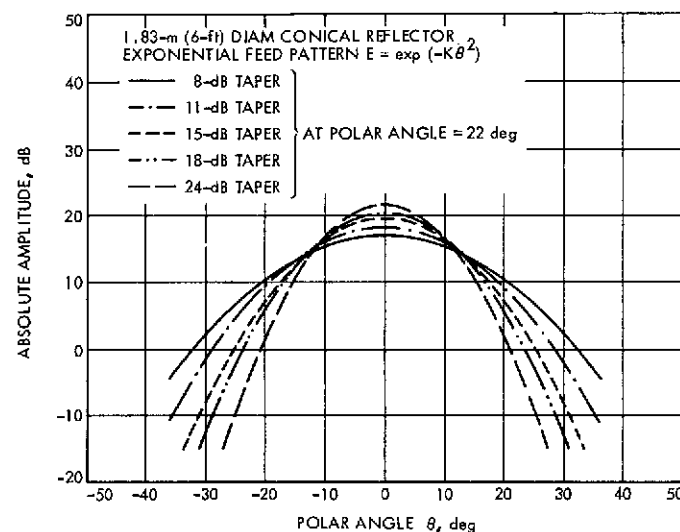


**Fig. 4. Exponential feed patterns for quadreflex antenna**

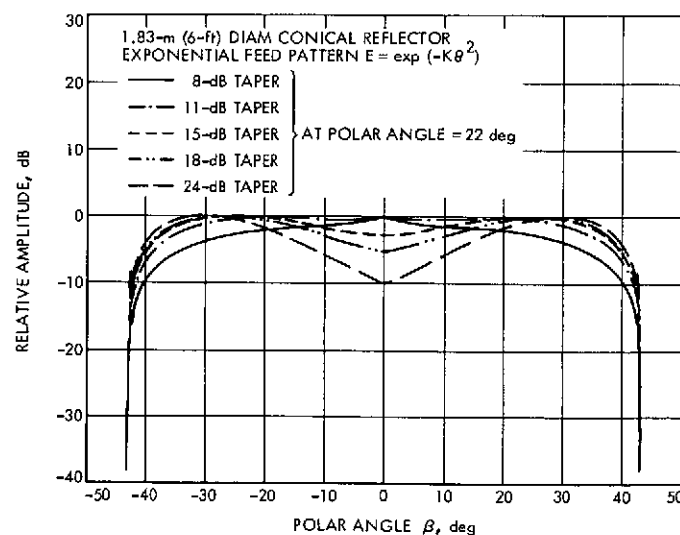


**Fig. 5. Aperture fields for quadreflex antenna**

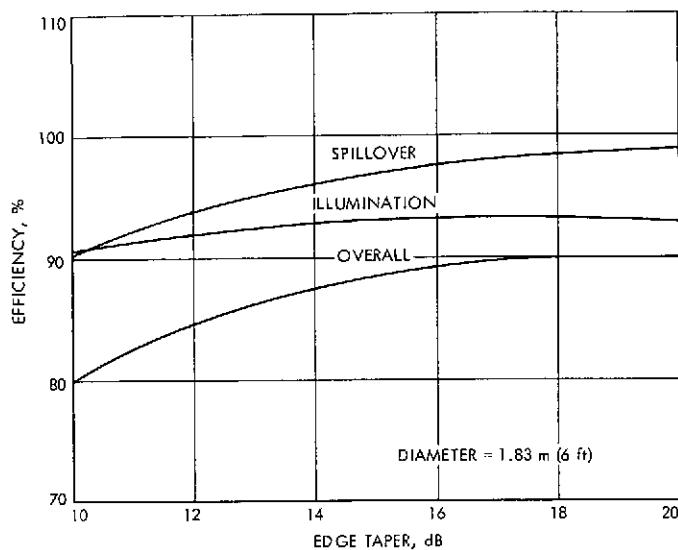


Fig. 6. Spillover, illumination, and overall efficiencies of quadreflex antenna

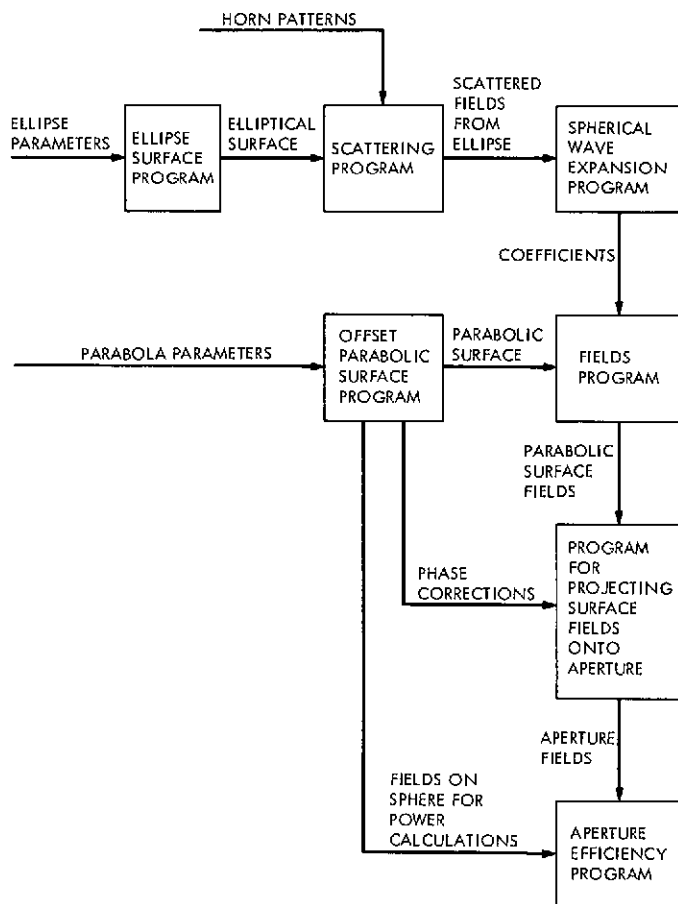
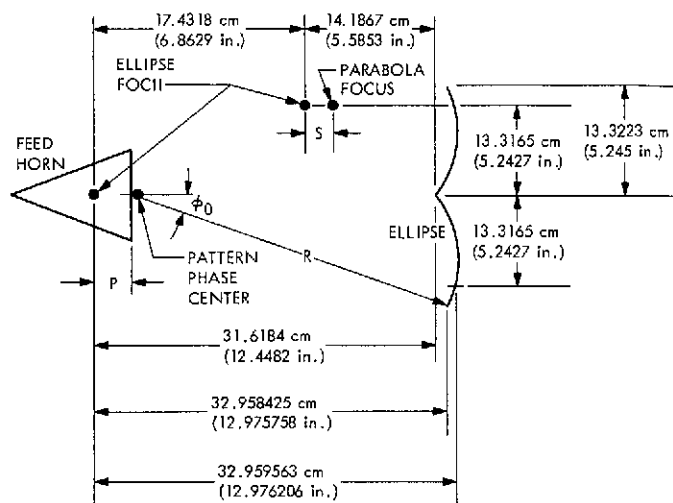


Fig. 7. Flow diagram of computer programs for calculating efficiency



FREQUENCY	POSITION	P, cm (in.)	S, cm (in.)	R, cm (in.)	$\phi_0$ , deg
KU-BAND	OPTICAL	2.125218 (0.8367)	0.0	33.586249 (13.223720)	23.368031
KU-BAND	MAX GAIN	5.704225 (2.245758)	0.0	30.336035 (11.943321)	26.050143
X-BAND	MAX GAIN	12.943225 (5.095758)	0.2032 (0.08)	24.043541 (9.465961)	33.648099

OTHER PARAMETERS (SEE FIG. 2)

$A = 13.3165$ cm (5.2427 in.)	$2a = 51.075803$ cm (20.108584 in.)
$\beta_0 = 43.187755^\circ$ FOR $\theta = 0.0$	$\phi = 37.376899^\circ$
$F = 98.6912$ cm (38.8548 in.)	$c = 10.968073$ cm (4.318139 in.)
$F/D = 0.631635$	$D = 365.76$ cm (144.0 in.)

Fig. 8. Subreflector and feed parameters

A series of aperture distributions were calculated for edge tapers between 9 and 20 dB, and the aperture efficiencies were in turn calculated from these distributions. Since ideal feed patterns with spherical phase fronts were considered, the phase was constant across the aperture and, therefore, did not contribute to any efficiency degradation. The spillover, illumination, and overall efficiency is plotted in Fig. 6. As can be seen, the overall efficiency increases rapidly from 9-dB edge tapers to about 14 dB and then levels out. The broad efficiency peak results from the fact that the spillover efficiency is improving at the same rate the illumination efficiency was decreasing. In measured efficiencies versus edge taper, the overall efficiency begins to drop off at about 14 to 15 dB. The difference is attributed to the fact that feed patterns in reality do not have ideal phase patterns. For most patterns the phase patterns begin to change rapidly, as the pattern amplitude drops. For cases where increased edge tapers are used, it would then be expected that over a greater portion of the aperture there would be widely varying phase values. The varying phase would then detract from the phase efficiency. Thus, if the efficiency computed from calculated aperture fields could be adjusted for phase, it would be expected to show the same dropoff observed from measured efficiencies.

### III. Efficiency Determined by Scattering Calculations

Because of the relatively small sizes of antennas under consideration, the various scattering surfaces were in the near field of the fields incident upon them. Therefore, using ray optics techniques does not provide sufficient accuracy. The approach taken to obtain a more rigorous

solution was to use the asymmetrical scattering program to obtain the scattered fields from the elliptical subreflector when the subreflector is illuminated by a corrugated horn. Then, by taking a spherical wave expansion of the scattered fields, the fields on the surface of the equivalent parabola were calculated and then projected onto the antenna aperture. Last, the antenna efficiency was then calculated based on the projected fields in the aperture plane. Figure 7 shows a flow chart describing the sequence of programs used to obtain the final efficiency value. Table 1 shows the efficiencies obtained for X-band and Ku-band antennas, each with a two-section corrugated horn feed. In each case the feed was located at the position that was experimentally found to give the highest efficiency. As a final case, the Ku-band configuration was adjusted to place the phase center at the focus of the ellipse. The efficiency that resulted is also presented in Table 1. Figure 8 shows the subreflector dimensions for each of the three cases.

Table 1. Antenna efficiency (1.83-m (6-ft) diameter)

Frequency	Ku-band	Ku-band	X-band
Feed phase center location	Optical	Maximum gain	Maximum gain
Efficiency			
Subreflector blockage	0.979	0.979	0.979
Spillover, main reflector	0.884	0.906	0.825
Urn blockage	0.972	0.987	0.989
Illumination	0.886	0.905	0.904
Phase	0.984	0.933	0.967
Overall	0.734	0.740	0.698

## References

1. Oliver, R. E., and Wilson, A. H., *Furlable Spacecraft Antenna Development: An Interim Report*, Technical Memorandum 33-537, pp. 6-7, Jet Propulsion Laboratory, Pasadena, Calif., Apr. 15, 1972.
2. Ludwig, A., Woo, K., Gustincic, J., and Hardy, J., "Recent Development of Conical Reflector Antennas", IEEE G-AP 1973 International Symposium Record, pp. 314-317, Aug. 1973.